Simulation Based Study of Wireless RF Interconnects for Practical CMOS Implementation

Ankit More
Drexel University
Department of Electrical and Computer Engineering
am434@drexel.edu

Baris Taskin
Drexel University
Department of Electrical and Computer Engineering
taskin@coe.drexel.edu

ABSTRACT

An electromagnetic analysis for the practical implementation of on-chip antennas to be used as wireless IC interconnects is presented. The undesired electromagnetic signal coupling between the on-chip antennas and the metal interconnects is characterized under varying geometries and placement of the metal interconnects. The variations in the transmission gain between the antenna pair due to the typical complementary metal oxide semiconductor (CMOS) manufacturing requirements are presented. Using a 3-D finite element method (FEM) based full wave electromagnetic solver, it is shown that the antenna characteristics are significantly impacted by the presence of the essential epitaxial layer and the required minimum metal utilization. It is also shown in a 250 nm CMOS technology that there can be a significant electromagnetic signal coupling between the on-chip transmitting antenna and the metal interconnects on a die (-12.09 dB for a 1.6 mm long, 2 μm wide interconnect at a distance of 1 μm from the antenna). Design considerations are presented for the metal interconnects in the presence of on-chip antennas in order to minimize the undesired electromagnetic signal coupling.

Categories and Subject Descriptors

B.4.3 [**Hardware**]: Input/Output and Data Communications—*Interconnections*

General Terms

Design

Keywords

VLSI, interconnects, on-chip antennas, electromagnetic

1. INTRODUCTION

The need for an alternative global IC interconnect system is growing to address the increasing concerns of timing, power and area overheads [1]. One possible alternative for a global communication network on a chip is to use radio frequency (RF) interconnects. There are two (2) types of RF IC interconnects of note: The micro-strip transmission line based interconnects operating in the RF range [2] and the wireless communication based intra-chip interconnects operating in the RF range [3]. This paper focuses on the latter. The high operating frequencies of the metal oxide semiconductor field effect transistor (MOSFET) devices have enabled the miniaturization and fabrication of antennas on-chip, enabling wireless IC interconnects.

There is a limited body of work on the design, analysis and manufacturing of on-chip antenna pairs for intra-chip communication [3–6]. The feasibility of establishing an intra-chip wireless communication channel using on-chip antennas for the global delivery of the clock signal has been shown in [3]. In order to minimize the cost of integrating wireless RF interconnects using on-chip antennas to IC design, the design of the antennas should adhere to the CMOS manufacturing process requirements. The lithographic limitations (or recommended alignment) on metal geometries of Manhattan-routing are ignored in [3, 4, 6], where antenna implementations with bend angles are proposed. Furthermore, the simulation models in [5, 6] do not include the epitaxial layer, which is shown to significantly impact the antenna radiation in this paper.

In [6], a simulation based analysis of the effect of the presence of metal interconnects on the antenna characteristics is performed. However, only a few metal interconnects are used in the model in [6], which is a very low percentage utilization of the metal layers. Metal utilization at these extremely low rates is not typical of most ICs as a minimum percentage utilization of the metal layers is required by the manufacturing process. The signal coupling for the wireless communication channel between the transmitting and the receiving antenna is due to wave propagation—not due to conduction through the substrate. The dominant path for wave propagation is through the same metal layer as that of the antennas. Hence, the presence of a high density of metallic structures can influence the signal coupling between the transmitting and the receiving antennas. Therefore, it is necessary to characterize the performance of the on-chip antennas under typical metal utilization factors. The observation that the signal coupling between the antennas is due to wave propagation also necessitates the analysis of the electromagnetic coupling between the on-chip antennas and the metal interconnects, which is lacking in the literature.

One contribution of this paper is in characterizing the effect of the (intra-chip communication) antenna radiation

SLIP'10, June 13, 2010, Anaheim, California, USA.

on the metal interconnects. Further, this work studies the feasibility of integrating antennas on chip using a standard foundry process. The following scenarios are studied to investigate these points:

1. The effects of the electromagnetic radiations from the antennas on the metal interconnects considering:
   (a) Interconnects at different metal layers (M1–M3),
   (b) Varying widths of the interconnect,
   (c) Varying lengths of the interconnect,
   (d) Varying distance of the interconnects from the transmitting antenna.
2. The effects of the typical CMOS manufacturing processes on the antenna design and characteristics:
   (a) Adherence to 90° bend angles on antennas,
   (b) Presence of a high-conductivity epitaxial layer in the simulation model,
   (c) Varying metal utilization factor.

The effects of the electromagnetic radiations are studied in order to evaluate the impact of antenna radiation on the metal interconnects of varying geometries for signal integrity concerns. The effects of a typical CMOS manufacturing process are integrated in order to develop an accurate simulation model for the feasibility study of the IC antennas.

2. LITERATURE REVIEW

The previous body of work can be categorized into three categories in relevance to the work presented in this paper:

1. Different antenna topologies [3–6].
2. Design principles of wireless interconnects in multi-metal layer semiconductor technologies [7, 8].
3. Analysis of wave propagation on an IC die [4, 9].

It is shown in [3–6] that the transmission gain between the antenna pairs can be improved by using different antenna topologies. In [3, 4], it is shown that among the various dipole antenna topologies, the zigzag antenna with a bend angle of 30° provides relatively high gains. However, these bend angles are not allowed in all CMOS manufacturing processes. The results in [3, 4] also show that the performance of the meander dipole antennas is very close to that of the zig-zag dipole antennas, so performance degradation of the antenna operation due to the rectilinear metal routes is minimal. The work presented in [3–6] also does not include the high conductivity epitaxial layer (p-type or n-type silicon). The epitaxial layer is essential to CMOS design as the circuit devices are present in this layer. Due to its high conductivity, the epitaxial layer can change the antenna characteristic and induce higher losses.

In [6], it is shown that the presence of metal interconnects placed on the same layer as that of the antenna in parallel orientation to the antenna decreases the antenna gain in the lower frequency range and increases it in the mid-band and high frequency ranges. However, the change in the gain is not very large and does not have a major influence on the transmission gain. In other words, the presence of the metal interconnects shifts the response to a higher frequency range. However, [6] does not analyze the effect of the radiation from the antennas on the local metal interconnects.

Table 1: Material characteristics of different silicon regions on a die.

Material	Conductivity (S/m)	Relative Permittivity
Silicon Dioxide	0	3.7
20 Ω-cm Substrate (lightly doped)	5	11.9
P-type Silicon	800	11.9
N-type Silicon	2300	11.9
P^+/N^+ (active regions)	62500	11.9

Since there are local interconnects present in the same metal layer as that of the antenna, substantial amount of power can be transmitted to these interconnects from the radiations. Hence, it is critical to analyze the transmission gain between the antenna and the local interconnects. Since the interconnects are essentially micro-strip elements, the signal coupling depends on the dimensions of the interconnect.

In [7] and [8], it is shown that the presence of metal interconnects directly above or below the antenna structures significantly reduces the gain of the antennas. This is because of the undesirable reflection of the dipole antenna formed in these metal layers. In [4] and [9], it is shown that the majority of the wave propagation happens in the substrate and through surface waves. This increases the criticality of the analysis of the effect of the radiation on the metal interconnects in the same metal layer as that of the antenna. The intensity of the radiation is the highest on the surface containing the antenna and the metal interconnects, and through the substrate which contains the transistors.

The effect of the radiation on the local metal interconnects is important as it can impact the overall behaviour of a system using wireless interconnects for intra-chip communication. In particular, the effect of the radiation on the metal interconnects can interfere with the integrity of the signals on the metal interconnect. The criticality of the antenna electromagnetic radiation effects on the metal interconnects significantly increases for deep sub-micron technologies as V_{DD} and noise margins for these technologies are scaled down significantly.

3. WIRELESS INTERCONNECT ANALYSIS

The electromagnetic radiation effects of the wireless interconnect system on a die are investigated using an FEM-based full-wave simulation analysis. In particular, the wireless interconnect system is analyzed for the coupling of the transmitting and receiving antennas as well as the (undesirable) coupling between the transmitting antenna and the metal interconnects. The simulation of the wireless interconnect system is performed in Ansoft HFSS (High Frequency Structure Simulator) [10], a 3-D FEM based simulator. The design parameters for the die are selected according to a typical 250 nm CMOS technology manufactory data. Conductivity parameters of this 250 nm CMOS technology are presented in Table 1 [11]. The antenna characteristics depend on the operating environment of the on-chip antenna pair. For a CMOS process with a large number of metal layers [e.g. a nine (9) metal layer process], placing the antenna

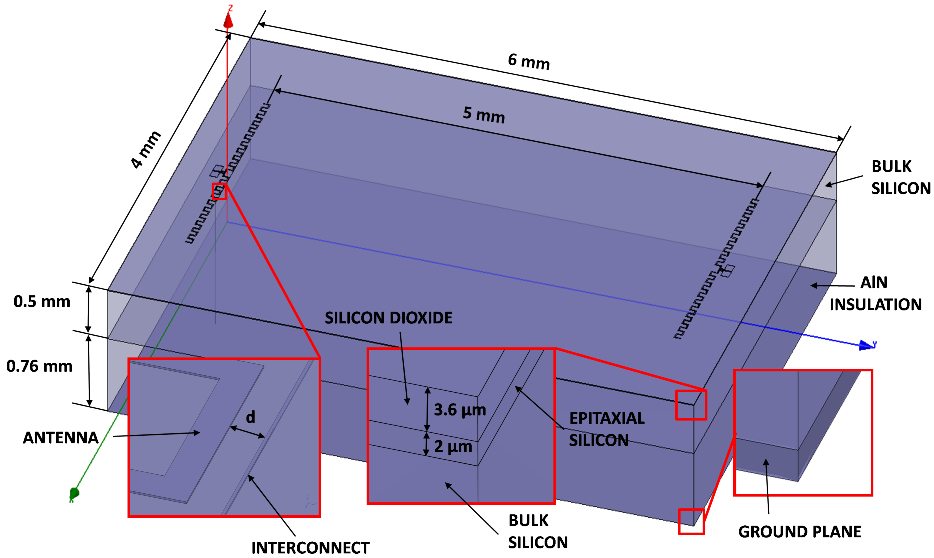

Figure 1: Simulated structure for the wireless interconnect system. Design dimensions are according to a typical 250 nm design technology.

Table 2: Dimensional parameters of the simulation model of the die.

Design Parameter	Magnitude
Die Length	6 mm
Die Width	4 mm
Silicon Dioxide Thickness (Epitaxial Layer to M3 Layer)	3.6 μm
Epitaxial Silicon Thickness	2 μm
Bulk Silicon Thickness	0.5 mm
Aluminium Nitride Insulation Thickness	0.76 mm
Ground Plane Thickness	2 μm

Table 3: Dimensional parameters of the meander dipole antenna.

Design Parameter	Magnitude
Arm Length (excluding bend lengths)	1.2 mm
Arm Run Length (including bend lengths)	2.4 mm
Bend Element Width	10 μm
Bend Element Length	60 μm
Antenna Thickness (M3 Thickness)	0.6 μm

on the last metal layer (e.g. M9 metal layer) will increase the separation of the antenna from the lossy substrate, thereby, improving the antenna characteristics.

The simulation model is shown in Figure 1. The die size is arbitrarily selected as 6 x 4 mm^2 where the antennas are separated at a distance of 5 mm from each other. In the 3-metal layer 250 nm process, the antennas are placed in the third metal layer. In Figure 1, the placement of the interconnect is also shown at a distance d from the transmitting antenna. The material of the epitaxial silicon is varied to study its effect on the antenna characteristics. The dimensions and the placement of the interconnect are varied in order to evaluate the impact of antenna radiation on the metal interconnects of varying geometries for signal integrity concerns.

Meander dipole antennas are used in the simulation model as these antennas are more compatible with conventional CMOS technologies in having 90° bend angles (i.e. Manhattan-routing). The antennas are designed to operate at 17 GHz with a total arm length (including the length of the meander segments) of 2.4 mm according to the parameters presented in [12]. The operation frequency of 17 GHz is chosen arbitrarily and is not the highest or the lowest possible operating frequency. However, the choice of a lower operating frequency would require a larger antenna dimension and therefore occupy a larger die footprint. The wavelength λ of the radiated electromagnetic waves is 6.85 mm based on an effective dielectric constant $\epsilon_r = 6.61$ [13]. For the reproducibility of the results, the dimensions of the die and the antennas are provided in Table 2 and Table 3, respectively.

The following impacts of the geometry and placement of the metal interconnects on the coupling between the antenna and the interconnect are studied:

1. Impact of interconnects in different metal layers (3 metal layer process),
2. Impact of varying width of interconnects from 2 μm to 10 μm (all three metal layers),
3. Impact of varying length of interconnects from 100 μm to 3200 μm (M3 layer),
4. Impact of varying distance of interconnects from the transmitting antenna from 1 μm to 4.5 mm (M3 layer).

In items 3 and 4, a 2 μm wide, M3 interconnect is used since it is the worst case observed in items 1 and 2. Analysis of the metal utilization factor is performed with arbitrarily varying percentage metal utilizations of the third metal layer. As it will be shown in Section 4, the epitaxial layer has a significant affect on the electromagnetic characteristics of the system on the die. Hence, the above items are simulated with a p-type epitaxial layer as it is commonly used in most standard CMOS processes.

The metal interconnects are placed parallel to the antenna. This is such, as the gain for the dipole antenna is highest in the direction perpendicular to the antenna and at the center of the antenna structure. Experimentally, the highest antenna gain leads to the modelling of the worst case of the interference effects for the interconnects. The simulations are performed in the frequency range from 10 GHz to 30 GHz as the target operating frequency is 17 GHz.

4. SIMULATION RESULTS

The simulation results for the various cases outlined in Section 3 are presented in Sections 4.1, 4.2 and 4.3.

In experimentation, two primary sets of data are collected:

1. The scattering parameter (s-parameter) matrix between the antenna pair, **S**.
2. The transmission s-parameter between the transmitting antenna and the metal interconnects, S_{i1}.

The s-parameter matrix **S** between the antenna pair is used to characterize the operation of the wireless communication system of the intra-chip wireless interconnect. The s-parameter S_{11} (also defined as the radiation loss) characterizes the radiation frequency of the transmitting antenna and the parameter S_{21} characterizes the signal coupling between the radiating and the transmitting antennas. The return loss of the transmitting antenna depicts the frequencies at which the antenna will radiate energy efficiently. It is desirable that the return loss be high for the desired bandwidth of frequencies to be transmitted and low for all other frequencies. The transmission gain between the antennas is the figure of merit used to characterize the strength of the signal coupling between the transmitting and receiving antennas. The transmission gain G_a of the antenna pair is given by:

$$G_a = \frac{|S_{21}|^2}{(1-|S_{11}|^2)(1-|S_{22}|^2)} \quad (1)$$

where S_{21} is the forward transmission, S_{11} is the reflection of the electric field at the transmitting antenna and S_{22} is the reflection of the electric field at the receiving antenna. In simulation, the s-parameter matrix **S** is computed, which is used to determine the three parameters S_{11}, S_{21}, and S_{22}. The transmission gain G_a is computed using (1).

4.1 Effects of the Epitaxial Layer on the Antenna Characteristics

The antenna radiates energy most efficiently in the frequency range where the magnitude of the return loss is the highest. The return loss for the transmitting antenna is depicted in Figure 2, where the most efficient frequency range for the simulation model without the epitaxial layer is 18.4 GHz. Such a simulation model without the epitaxial layer is used in previous works [5–7]. As discussed in Section 3, the epitaxial layer exists in most CMOS processes. The existence of this epitaxial layer shifts the operating frequency to 14.6 GHz and 12.6 GHz for the p-type and n-type epitaxial layer, respectively. This is not critical for the operation—as the return losses are still very high—but is essential for the accuracy of the estimation and simulation models. The high conductivity epitaxial layer also affects

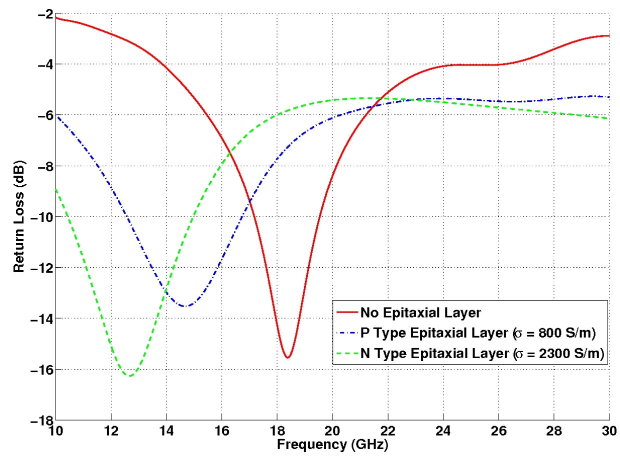

Figure 2: Return loss at the transmitting antenna for different epitaxial layers.

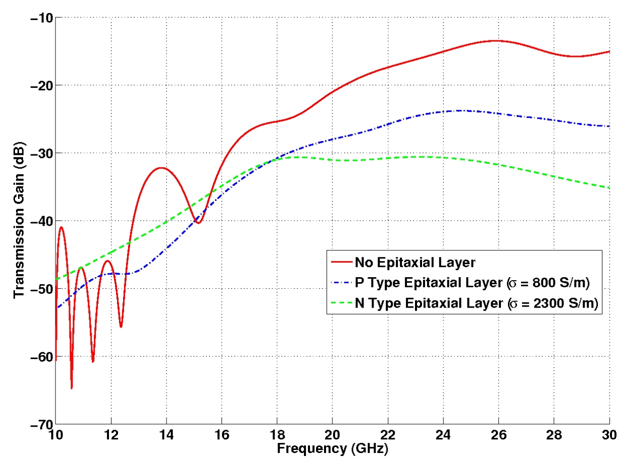

Figure 3: Transmission gain between the antenna pair for different epitaxial layers.

the transmission gain of the antenna pair as shown in Figure 3. The transmission gain is reduced by approximately 6 dB at the target frequency of 17 GHz which is a significant reduction in signal coupling. In order to have a functional communication channel, the transmission gain between the antenna pair should be higher than the gain provided by the low noise amplifier (LNA) at the receiver end. LNAs are capable of providing a gain of up to 50 dB. However, if the LNA is designed based on the simulation results without considering the epitaxial layer, then the presence of the epitaxial layer will reduce the transmission gain. If the reduction in transmission gain is large enough, then the communication link between the receiver and transmitter end can be disrupted. Therefore, unlike previous works, it is essential to include the epitaxial layer for correct modeling of the environment of operation for the on-chip antennas.

The percentage change in the transmission gain in the presence of the epitaxial layer at the target frequency is shown in Table 4. Between the p-type and n-type epitaxial layers, it is more desirable to use the p-type epitaxial layer for on-chip wireless interconnects both for the transmission gain and bandwidth considerations. Note that the p-type

Table 4: Percentage change in the transmission gain between the antennas for different epitaxial layers.

Epitaxial Layer	Transmission Gain (dB)	% Change in the Transmission Gain
No epitaxial layer	−26.75	–
P-type%	−33.10	23.74%
N-type%	−32.52	21.57%

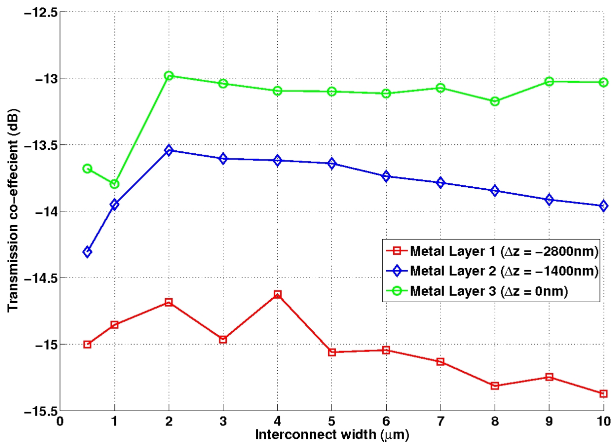

Figure 4: Signal coupling between the interconnect and the transmitting antenna for varying interconnect widths.

epitaxial layer is used for all simulations in this work with the frequency of operation at 14.6 GHz as it is the more common of the two in standard CMOS processes. The antenna radiates most efficiently (with the lowest return loss) at 14.6 GHz. The highest radiation efficiency of the antenna implies that the power of the electromagnetic radiations is the highest. Hence, the worst case electromagnetic coupling between the metal interconnect and the transmitting antenna on a die implemented with the p-type epitaxial layer is expected to be at this frequency (=14.6 GHz).

4.2 Electromagnetic Coupling Between the Antenna and the Interconnects

It is desired that the signal coupling between the transmitting antenna and the metal interconnect be low to avoid any signal integrity issues on these interconnects. The simulation results for the coupling between the metal interconnects and the transmitting antenna show substantial variations under different geometrical sizes and placement.

4.2.1 Variation with Width and Metal Layer

The transmission s-parameter between the transmitting antenna and a 1 mm long metal interconnect placed at a distance of 1 μm from the transmitting antenna, shown in Figure 4, is used to characterize the signal coupling between the two structures. The transmitting antenna is placed on the M3 metal layer and the placement of the interconnect is varied from M1 to M3. The signal coupling between the transmitting antenna and the interconnect decreases with increased metal layer separation between the two structures. The percentage change in the signal coupling between the

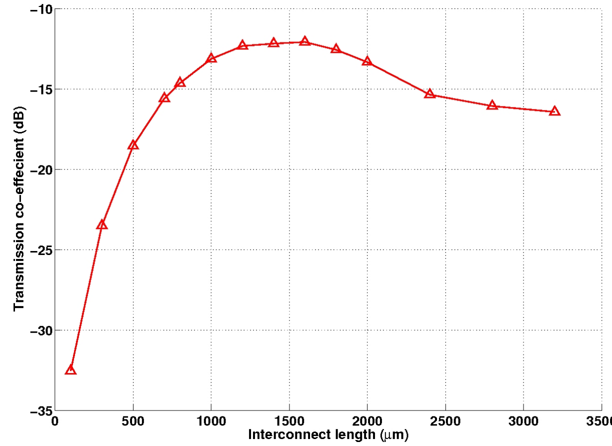

Figure 5: Signal coupling between the interconnect and the transmitting antenna for varying interconnect lengths.

interconnect and the transmitting antenna for placement in different metal layers is shown in Table 5. Note that the coupling is highest at an interconnect width of 2 μm for placement in all three metal layers. The irregularity in the decreasing trend past an interconnect width of 2 μm is due to convergence issues in numerical analysis methods. Nonetheless, the variation in the transmission s-parameter is not very large with a variation in the width of the metal interconnect (approximately 0.5 dB). Thus, the width of the interconnects does not have a major impact on the signal coupling: Wire sizing can be performed in integrated circuits with wireless interconnects.

4.2.2 Variation with Length

The s-parameter between the antenna and the M3 interconnect for varying lengths of a 2 μm wide interconnect placed at a distance of 1 μm from the transmitting antenna is shown in Figure 5. It is observed that the signal coupling is low for small lengths of the interconnects and peaks for lengths at about a quarter of the wavelength (=6.9/4 $\simeq$ 1.7 mm) of operation. At a quarter wavelength ($\simeq$1.7 mm), the interconnect is behaving as a quarter wave printed monopole antenna [13]. Due to the principle of reciprocity [13], the interconnect also *receives* the maximum amount of energy at this length. The signal coupling is alarmingly high for interconnects longer than 500 μm, however, note that such long lengths of interconnects are generally avoided in high speed integrated circuits. Further, if long interconnects exist they are typically buffered with repeaters, so the coupling impact is low. Note that, depending on the frequency of operation, the wavelength of the electromagnetic waves changes. Therefore, the length of the interconnect (quarter of the wavelength of electromagnetic waves), at which the signal coupling peaks, would also change. For the tested communication frequencies, the length of the metal interconnects typically employed in integrated circuits would not lead to significant signal integrity problems.

4.2.3 Variation with Distance from Antenna

The effect of varying the distance of a 2 μm wide, 1 mm long M3 interconnect from the transmitting antenna is shown in Figure 6. It is observed that the signal coupling decreases

Table 5: Percentage change in the transmission s-parameter between the transmitting antenna and the metal interconnect for different metal layer placements.

Metal Layer	Distance from the Antenna Layer (nm)	Transmission S-parameter (dB)	% Change in the Transmission S-parameter
M3	0	−12.98	–
M2	−1400	−13.54	4.31%
M1	−2800	−14.69	13.17%

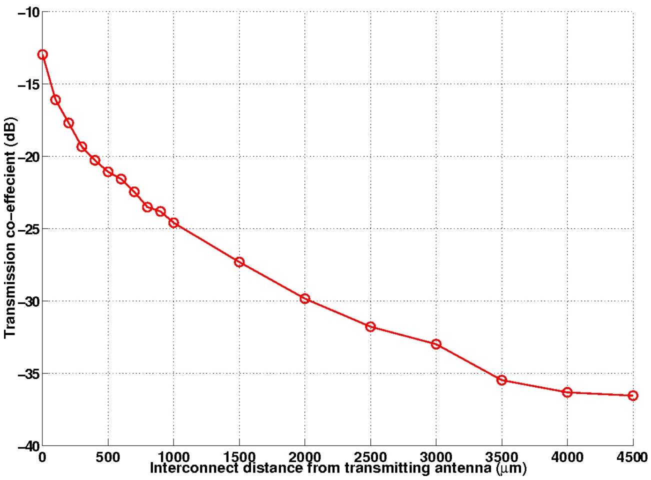

Figure 6: Signal coupling between the interconnect and the transmitting antenna for varying distance of the interconnect from the transmitting antenna.

monotonously with increasing distance from the transmitting antenna. The results for this case are explained using an alternative form of (1). The transmission gain G_a in (1) can also be computed analytically as:

$$G_a = \frac{|S_{21}|^2}{(1-|S_{11}|^2)(1-|S_{22}|^2)} = G_t G_r \left(\frac{\lambda}{4\pi R}\right)^2 e^{-2\alpha R} \quad (2)$$

where, G_t and G_r are the gains of the transmitting and receiving antennas, respectively, λ is the wavelength of the electromagnetic waves based on the effective dielectric constant ϵ_r, α is the attenuation constant and R is the separation between the transmitting and receiving antennas. In (2), the transmission gain G_a is inversely proportional to the separation R. Even though the interconnect is not an antenna, the strength of the electromagnetic waves reduces with distance from the antenna, and therefore the coupling between the antenna and the interconnect decreases with an increasing distance. At the tested frequency, worst-case interconnects in 500 μm proximity of the antennas experience up to −20 dB of undesirable coupling. Nonetheless, this level of coupling is not critical on most digital signals. Signals that are sensitive to noise should be routed outside the 500 μm radius of the transmitting antenna.

4.3 Effects of the Metal Utilization Factor on the Antenna Characteristics

Most CMOS foundry processes require a minimum metal utilization factor of 20% and allow a maximum metal utilization of 80%, hence, the simulations for the varying percentage metal utilization are performed in this range. The simulation results for the metal utilization of the same metal

Table 6: Percentage change in the transmission gain between antenna pair for different metal utilization.

% Metal Utilization	Transmission Gain (dB)	% Change in the Transmission Gain
0% (no metal)	−33.10	–
22%	−33.24	0.42%
49%	−32.93	−0.51%
73%	−37.98	14.74%
83%	−41.57	25.59%

layer as that of the antennas is shown in Figure 7. The frequency range of operation (observed at the tip of the return loss) as shown in Figure 7(a), shows a very small variation with percentage utilization. However, the transmission gain is reduced substantially with a high percentage metal utilization as shown in Figure 7(b). The percentage change in the transmission gain between the antenna pair is only 0.51% up to a metal utilization of 49% for M3. However, for higher values of percentage utilization, the change in transmission gain is very large and might cause the failure of the wireless link between the antenna pair. The large reduction in the transmission gain is due to very high interference from the metal structures effectively shielding the receiving antenna from the electromagnetic surface waves, which is the dominant mode of wave propagation (as explained in Section 2). The change in the transmission gain depicted in Figure 7(b) is tabulated in Table 6. In general, the effect of the metal utilization on the antenna characteristics can change the field distribution, which can either effect the coupling between the transmitting and receiving antenna favourably or adversely.

5. RESULTS AND CONCLUSIONS

The presented results can be summarized as follows:

1. The presence of the essential high conductivity epitaxial layer reduces the transmission gain between the antenna pair by ∼6 dB (Figure 3 and Table 4).

2. There can be substantial amount of coupling between the transmitting antenna and the metal interconnects. The coupling:

   (a) Decreases with placement in different metal layers. Lower coupling for higher separation of metal layers (Figure 4 and Table 5),

   (b) Remains approximately constant with varying width of the interconnect. Peaks at interconnect width of 2 μm but variations are very low (approximately 0.5 dB) (Figure 4),

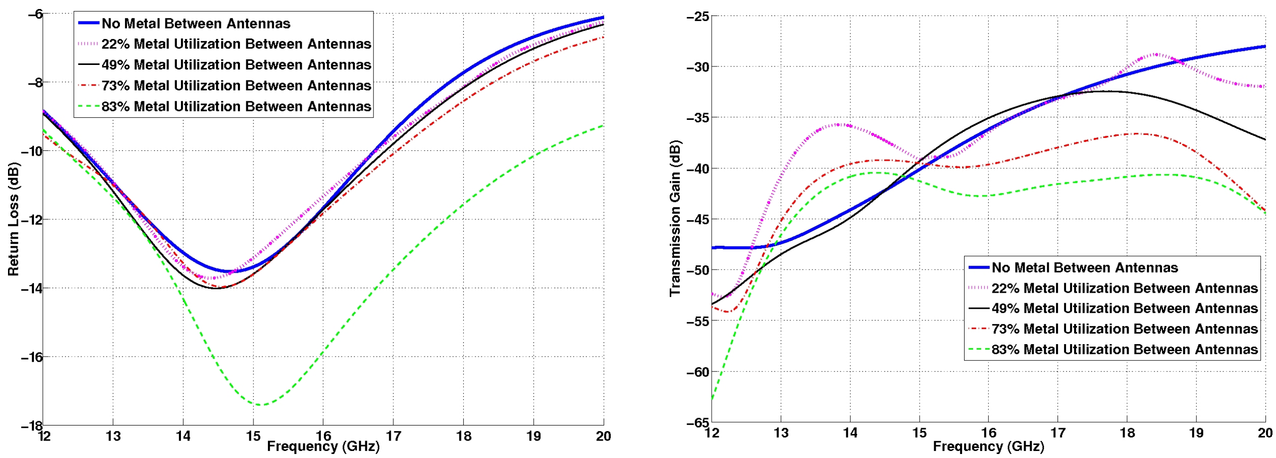

(a) Return Loss. (b) Transmission Gain.

Figure 7: Antenna characteristics for varying percentage utilization of M3.

- (c) Is very low at small interconnect lengths. Peaks at interconnect length of approximately quarter of the wavelength of the EM waves (Figure 5),
- (d) Monotonously decreases with increasing distance from the transmitting antenna (Figure 6).

3. The transmission gain between the antenna pair varies depending on the percentage utilization of same metal layer of the antenna. The variation is low up to 49% metal utilization and substantial for higher values of percentage metal utilization (Figure 7 and Table 6).

The coupling between the interconnects and the transmitting antenna is undesirable and can cause signal integrity problems depending on the geometry of the interconnect. The effect of the electromagnetic coupling between the antenna and the interconnects on the device operation has to be evaluated. In particular, the device operation has to be studied for any faulty switching caused by the electromagnetic coupling between the antenna and the interconnects.

These results show that it is possible for the radio frequency (RF) wireless interconnects system to have a good electromagnetic compatibility and low electromagnetic interference with the metal interconnects on a die. The design considerations for the interconnect geometry and placement with respect to the antenna specifications must be integrated into the physical design automation processes.

6. REFERENCES

[1] *ITRS International Technology Roadmap for Semiconductors*, 2006.

[2] M. F. Chang, V. P. Roychowdhury, L. Zhang, H. Shin, and Y. Qian, "RF/wireless interconnect for inter- and intra-chip communications," *Proceedings of the IEEE*, vol. 89, pp. 456–466, April 2001.

[3] B. A. Floyd, C. M. Hung, and K. K. O, "Intra-chip wireless interconnect for clock distribution implemented with integrated antennas, receivers and transmitters," *IEEE Journal of Solid-State Circuits*, vol. 37, pp. 543–551, May 2002.

[4] K. Kim, "Design and characterization of RF components for inter- and intra- chip wireless communication," Ph.D. dissertation, University of Florida, 2000.

[5] T. Kikkawa, K. Kimoto, and S. Watanabe, "Ultra wideband characteristics of fractal dipole antennas integrated on Si for ULSI wireless interconnects," in *IEEE Electron Device Letters*, vol. 26, October 2005, pp. 767–769.

[6] M. Bialkowski and A. Abbosh, "Investigations into intra chip wireless interconnection for ultra large scale integration technology," in *Proceedings of the IEEE Antennas and Propagation Society International Symposium (APSURSI)*, June, pp. 1–4.

[7] A. B. M. H. Rashid, N. Sultana, M. R. Khan, and T. Kikkawa, "Efficient design of integrated antennas on si for on-chip wireless interconnects in multi-layer metal process," *Japanese Journal of Applied Physics*, vol. 44, pp. 2756–2760, April 2005.

[8] E. Seok and K. K. O, "Design rules for improving predictability of on-chip antenna characteristics in the presence of other metal structures," in *Proceedings of the IEEE International Interconnect Technology Conference (IITC)*, June 2005, pp. 120–122.

[9] M. Sun, Y. P. Zhang, G. X. Zheng, and W. Y. Yin, "Performance of intra-chip wireless interconnect using on-chip antennas and UWB radios," *IEEE Transactions on Antennas and Propagation*, vol. 57, pp. 2756–2762, September 2009.

[10] *High Frequency Structure Simulator: User's Guide*, 10th ed., Ansoft Corporation, June 2005.

[11] S. Bronckers, K. Scheir, G. V. Plas, G. Vandersteen, and Y. Rolain, "A methodology to predict the impact of substrate noise in analog/RF systems," *IEEE Transactions on Computer-Aided Design of Integrated Circuit and Systems*, vol. 28, pp. 1613–1626, November 2009.

[12] H. Nakano, H. Tagami, A. Yoshizawa, and J. Yamauchi, "Sortening ratios of modified dipole antennas," *IEEE Transactions on Antennas and Propagation*, vol. 32, pp. 385–386, April 1984.

[13] D. M. Pozar, *Microwave Engineering*, 3rd ed. Wiley, 2005.